



**HAL**  
open science

## A model to predict modal radiation by finite-sized sources in semi-infinite isotropic plates

Mathilde Stévenin, Alain Lhémery, Sébastien Grondel

► **To cite this version:**

Mathilde Stévenin, Alain Lhémery, Sébastien Grondel. A model to predict modal radiation by finite-sized sources in semi-infinite isotropic plates. *Journal of Physics: Conference Series*, 2017, *Journal of Physics: Conference Series*, 797, 012005, 12 p. 10.1088/1742-6596/797/1/012005 . hal-03564111

**HAL Id: hal-03564111**

**<https://uphf.hal.science/hal-03564111>**

Submitted on 7 Feb 2024

**HAL** is a multi-disciplinary open access archive for the deposit and dissemination of scientific research documents, whether they are published or not. The documents may come from teaching and research institutions in France or abroad, or from public or private research centers.

L'archive ouverte pluridisciplinaire **HAL**, est destinée au dépôt et à la diffusion de documents scientifiques de niveau recherche, publiés ou non, émanant des établissements d'enseignement et de recherche français ou étrangers, des laboratoires publics ou privés.

PAPER • OPEN ACCESS

## A model to predict modal radiation by finite-sized sources in semi-infinite isotropic plates

To cite this article: M Stévenin *et al* 2017 *J. Phys.: Conf. Ser.* **797** 012005

View the [article online](#) for updates and enhancements.

You may also like

- [Overcoming analytic solution limitations in gravitational wave direction determination](#)  
C F Da Silva Costa and N S Magalhaes
- [Testing modified gravity at cosmological distances with LISA standard sirens](#)  
Enis Belgacem, Gianluca Calcagni, Marco Crisostomi *et al.*
- [Cosmological backgrounds of gravitational waves](#)  
Chiara Caprini and Daniel G Figueroa

**PRIME**  
PACIFIC RIM MEETING  
ON ELECTROCHEMICAL  
AND SOLID STATE SCIENCE

HONOLULU, HI  
Oct 6-11, 2024

Abstract submission deadline:  
**April 12, 2024**

Learn more and submit!

**Joint Meeting of**  
The Electrochemical Society  
•  
The Electrochemical Society of Japan  
•  
Korea Electrochemical Society

# A model to predict modal radiation by finite-sized sources in semi-infinite isotropic plates

M Stévenin<sup>1</sup>, A Lhémy<sup>1</sup> and S Grondel<sup>2</sup>

<sup>1</sup> CEA LIST, point courrier 120, bâtiment 565, 91191 Gif-Sur-Yvette Cedex, France

<sup>2</sup> IEMN-DOAE, UVHC, Le Mont Houy, 59313 Valenciennes Cedex 9, France

E-mail: [alain.lhemery@cea.fr](mailto:alain.lhemery@cea.fr)

**Abstract.** Elastic guided wave (GW) propagation is involved in various non-destructive testing (NDT) techniques of plate-like structures. The present paper aims at describing an efficient model to predict the GW field radiated by various sources attached at a distance of the straight boundary of an isotropic plate, a configuration often encountered in typical examinations. Since the interpretation of GW propagation and scattering in plates is made easier by the use of modal description, the model is derived in the classical theoretical framework of modal solutions. Direct radiation by a uniform source of finite size in an isotropic plate can be efficiently modelled by deriving Fraunhofer-like approximation. A rigorous treatment is proposed based upon i) the stationary phase method to describe the field after reflection at a plate edge, ii) on the computation of modal reflection coefficients for an arbitrary incidence relative to the edge and iii) on the Fraunhofer approximation to account for the finite size of the source. The stationary phase method allows us to easily express the amplitude of reflected modes, that is to say, the way waves spread, including reflections involving mode conversions. The computation of modal reflection coefficients for plane GW at oblique incidence was recently treated in the literature and our work for this very problem simply consisted in adapting it to the SAFE calculation we use to compute modal solutions.

The overall computation of the direct and reflected contributions is numerically very efficient. Once the total field is computed at a given frequency, the time-dependent field is obtained by simple Fourier synthesis.

## 1. Introduction

Nondestructive testing (NDT) of plate-like structures using elastic guided waves (GW) is the context of our work. Thanks to the ability of GW to propagate at long distances, one can perform fast inspections of large structures without the need for moving a transmitter and a receiver. When GW are generated by transducers of finite size, diffraction effects occur. Plate-like structures under examination are also of finite size so that GW generated in the plate can be reflected onto its edges. Since GW propagate as a series of differing modes, reflection of one GW at an edge can lead to mode-conversion phenomena.

Simulation is most helpful to help managing the complexity of GW propagation and scattering. To be realistic, transducer diffraction effects must be accounted for to accurately predict the wave-field radiated into the plate. The present work aims at proposing a model for predicting the field radiated by a finite-sized transducer into a plate of finite size, by considering as an elementary solution both the direct field radiated and the field after reflection at one straight

edge of the plate. In the literature, some models [1] which can be compared to Fraunhofer-like approximations have been developed for elastic guided waves in the case of isotropic and homogeneous plates, leading to fast computation of typical diffraction effects. In the Section 3.1, we present briefly the principle of Fraunhofer-like approximation. Thanks to the stationary phase method, an equivalent expression is obtained for the reflected field, which accounts for possible mode-conversion in the reflection process. The reflection at an edge of a plane GW are the subject of a few publications [2, 3] that we will use to calculate the reflection coefficients.

Finally simulation results are shown to illustrate the capabilities of our model.

## 2. General expression of the displacement field

We consider a semi-infinite plate as shown in Fig. 1, of thickness  $2d$ , which upper plane is at  $z = d$  and lower plane at  $z = -d$ . The plate is assumed to be made of an isotropic material. The plate edge is straight and belongs to the plane defined by the equation  $x = 0$ .

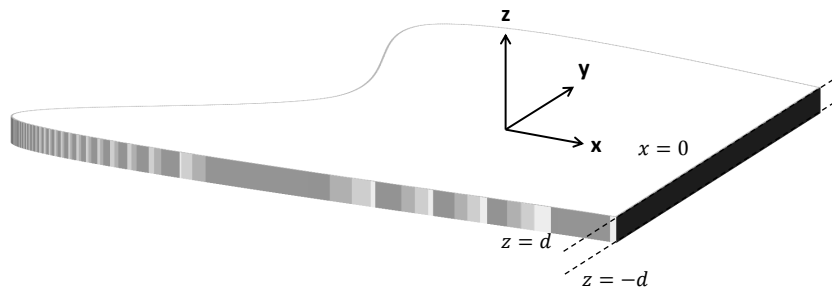


**Figure 1.** System geometry.

The total field  $\mathbf{u}$  radiated by the source is expressed in what follows as the sum of the direct field  $\mathbf{u}_d$  and the reflected field  $\mathbf{u}_r$ .

### 2.1. Direct field

The direct field radiated by a finite-sized source can be expressed in the form of a spatial convolution integral of a Green's function  $\mathbf{g}_d(x, y, z)$  with a source term  $\mathbf{q}(x, y)$ :

$$\mathbf{u}_d(x, y, z, \mathbf{q}) = \iint_S \mathbf{g}_d(x - x', y - y', z) \mathbf{q}(x', y') dx' dy'. \quad (1)$$

The expression of this Green's function can be found in the literature [4]. By introducing its expression into equation (1) the direct field in an isotropic plate can be expressed as a sum over the propagative modes,

$$\mathbf{u}_d(x, y, z, \mathbf{q}) = \sum_m \iint_S \left[ \frac{|k_m|}{2\pi} \frac{i\omega}{4P_m} \mathbf{V}_m(\varphi', z) \mathbf{V}_m(\varphi', d)^{*T} \mathbf{q}(x', y') \sqrt{\frac{2\pi}{|k_m|}} \right. \\ \left. \times e^{i\frac{\pi}{4} \text{sgn}(-k_m)} e^{ik_m \sqrt{(x-x')^2 + (y-y')^2}} \left( \sqrt{(x-x')^2 + (y-y')^2} \right)^{-1/2} \right] dx' dy'. \quad (2)$$

In this expression,  $k_m$  is the wave number of the mode  $m$ ,  $\varphi'$  is such that  $\tan \varphi' = \frac{y-y'}{x-x'}$ ,

$P_m$  is the average flow power of the mode  $m$ ,  
 and

$$\mathbf{V}_m(\varphi', z) = \mathbf{A}^{-1}(\varphi') \mathbf{W}^{(m)}(z),$$

is the displacement field distribution  $\mathbf{W}^{(m)}$  for the  $m$ th mode in the direction of propagation  $\varphi'$ , where  $\mathbf{A}$  is a rotation matrix allowing us to express the field in the plate coordinates,

$$\mathbf{A} = \begin{pmatrix} \cos \varphi' & \sin \varphi' & 0 \\ -\sin \varphi' & \cos \varphi' & 0 \\ 0 & 0 & 1 \end{pmatrix}.$$

The modal contributions are computed by means of the Semi Analytic Finite Element (SAFE) method [5].

### 2.2. Reflected field

In this section, the Green's function  $g_r$  for the reflected field is considered.

$$\mathbf{u}_r(x, y, z, \mathbf{q}) = \iint_S g_r(x - x', y - y', z) \mathbf{q}(x', y') dx' dy'. \quad (3)$$

As already done when considering the direct field, the reflected field  $\mathbf{u}_r$  is written as a sum over the different modal paths,

$$\mathbf{u}_r(x, y, z, \mathbf{q}) = \sum_m \sum_n \iint_S g_{rm,n}(x - x', y - y', z) \mathbf{q}(x', y') dx' dy', \quad (4)$$

where the subscript  $m$  denotes the mode considered for incident paths and  $n$  denotes the mode considered for reflected paths.

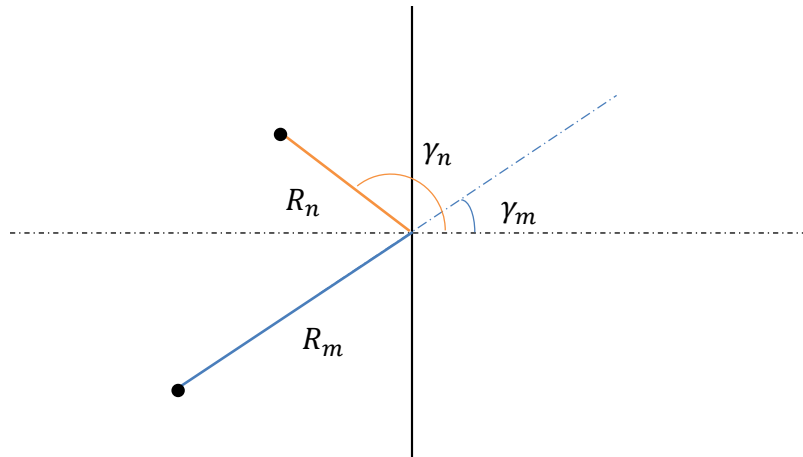


**Figure 2.** Notations.

Now, as point sources radiate a wavefield where waves spread with a cylindrical symmetry, wave amplitude decreases asymptotically as  $r^{-1/2}$  while their phase linearly depends on the distance from the source point. At this stage, to deal with the reflection upon the straight edge, it is interesting to decompose such a wavefield as a continuous spectrum of plane waves expressed

in relation to the edge position. To do this, we use Equation (28a) from Stamnes and Eide [6] and Equation (5.3a) from Stamnes [7], and after some algebra, we can obtain that

$$\sqrt{\frac{1}{kR}} e^{ikR} = \sqrt{\frac{i}{2\pi}} \int_{-\infty}^{\infty} \frac{e^{ikR}}{k_x} dk_y = \frac{1}{2\pi} \int_{-\infty}^{\infty} \frac{\sqrt{2i\pi}}{k_x} e^{ikR} dk_y. \quad (5)$$

So, a spectral elementary component of the wavefield from a point source has the following value  $\frac{\sqrt{2i\pi}}{k_x}$ . The Green's function expressing the reflected field along one of the paths  $m, n$  may be written as,

$$g_{rm,n} = \frac{1}{2\pi} \int G_{rm,n} \frac{\sqrt{2i\pi}}{k_{mx}} e^{i(k_{mx}(x_{m,n}-x') + k_{nx}(x-x_{m,n}) + k_y y)} dk_y, \quad (6)$$

where  $G_{rm,n}$  is an amplitude term which will be determined later.

$$g_{rm,n} = \sqrt{\frac{i}{2\pi}} \int G_{rm,n} \frac{e^{i(k_{mx}(x_{m,n}-x') + k_{nx}(x-x_{m,n}) + k_y y)}}{k_{mx}} dk_y. \quad (7)$$

The Green's function  $g_{rm,n}$  is now calculated thanks to the stationary phase method by expanding at second order the phase function about the direction of stationary-phase. For this, the second order derivative of the phase function must be calculated. The phase term has the following form,

$$f(k_y) = k_{mx}(x_{m,n} - x') + k_{nx}(x - x_{m,n}) + k_y y. \quad (8)$$

The second order Taylor's expansion about the path of stationary phase is

$$f(k_y) = f(k_{ys}) + \left. \frac{\partial f}{\partial k_y} \right|_{k_{ys}} (k_y - k_{ys}) + \frac{1}{2} \left. \frac{\partial^2 f}{\partial k_y^2} \right|_{k_{ys}} (k_y - k_{ys})^2, \quad (9)$$

In this expression, the first order derivative vanishes as the expansion is related to the path of the stationary phase. The second order derivative is the following,

$$\begin{aligned} \left. \frac{\partial^2 f}{\partial k_y^2} \right|_{k_{ys}} &= -\frac{(x_{m,n} - x')}{k_{mx}} \frac{1}{\cos^2 \gamma_m} - \frac{(x - x_{m,n})}{k_{nx}} \frac{1}{\cos^2 \gamma_n} \\ &= -\frac{1}{k_m} \frac{1}{\cos^2 \gamma_m} \left( R_m + R_n \frac{k_m \cos^2 \gamma_m}{k_n \cos^2 \gamma_n} \right), \end{aligned} \quad (10)$$

where, if  $(x_{m,n}, y_{m,n})$  denotes the point of the plate edge where reflection arise,

$R_m$  is the distance of this point to the source point.

Likewise,  $R_n$  is the distance between the calculation point and the point where reflection arises.

$\gamma_m$  and  $\gamma_n$  are the phase directions before and after reflection, respectively. We can now replace the phase with its development,

$$\begin{aligned} &\int_{-\infty}^{\infty} \frac{e^{i(k_{mx}(x_{m,n}-x') + k_{nx}(x-x_{m,n}) + k_y y)}}{k_{mx}} dk_y \\ &= \frac{e^{i(k_m R_m + k_n R_n)}}{k_{mx}} \int_{-\infty}^{\infty} e^{-i\frac{1}{2} \left( \frac{1}{k_m} \frac{1}{\cos^2 \gamma_m} \left( R_m + R_n \frac{k_m \cos^2 \gamma_m}{k_n \cos^2 \gamma_n} \right) \right) (k_y - k_{ys})^2} dk_y \end{aligned} \quad (11)$$

We recognize in this expression a Gaussian integral,

$$\begin{aligned} &\int_{-\infty}^{\infty} e^{-i\frac{1}{2} \left( \frac{1}{k_m} \frac{1}{\cos^2 \gamma_m} \left( R_m + R_n \frac{k_m \cos^2 \gamma_m}{k_n \cos^2 \gamma_n} \right) \right) (k_y - k_{ys})^2} dk_y \\ &= e^{-i\frac{\pi}{4} \operatorname{sgn} \left( \frac{1}{k_m} \left( R_m + R_n \frac{k_m \cos^2 \gamma_m}{k_n \cos^2 \gamma_n} \right) \right)} \sqrt{\frac{2\pi |k_m|^2 \cos^2 \gamma_m}{\left| R_m k_m + R_n k_n \left( \frac{k_m \cos \gamma_m}{k_n \cos \gamma_n} \right)^2 \right|}} \end{aligned} \quad (12)$$

So we have,

$$\int_{-\infty}^{\infty} \frac{e^{i(k_{mx}(x_{m,n}-x') + k_{nx}(x-x_{m,n}) + k_y y)}}{k_{mx}} dk_y = e^{i(k_m R_m + k_n R_n)} e^{-i\frac{\pi}{4} \operatorname{sgn}\left(\frac{1}{k_m} \left(R_m + R_n \frac{k_m \cos^2 \gamma_m}{k_n \cos^2 \gamma_n}\right)\right)} \sqrt{\frac{2\pi}{\left|R_m k_m + R_n k_n \left(\frac{k_m \cos \gamma_m}{k_n \cos \gamma_n}\right)^2\right|}} \quad (13)$$

$$g_{rm,n} = \sqrt{\frac{i}{2\pi}} e^{i(k_m R_m + k_n R_n)} e^{-i\frac{\pi}{4} \operatorname{sgn}\left(\frac{1}{k_m} \left(R_m + R_n \frac{k_m \cos^2 \gamma_m}{k_n \cos^2 \gamma_n}\right)\right)} \times G_{rm,n} \sqrt{\frac{2\pi}{\left|R_m k_m + R_n k_n \left(\frac{k_m \cos \gamma_m}{k_n \cos \gamma_n}\right)^2\right|}}. \quad (14)$$

Just before the reflection, the displacement field due to the  $m$  mode is given by,

$$\mathbf{u}_{dm}(x_p, y_p) = \left[ \frac{|k_m|}{2\pi} \frac{i\omega}{4P_m} \mathbf{V}_m(\varphi_m, z) \mathbf{V}_m(\varphi_m, d)^{*T} \mathbf{q}(x', y') \times \sqrt{\frac{2\pi}{|k_m R_m|}} e^{i\frac{\pi}{4} \operatorname{sgn}(-k_m)} e^{ik_m R_m} \right], \quad (15)$$

so that just after the reflection, the displacement field can be written as

$$\mathbf{u}_{rm,n}(x_p, y_p) = r_{m,n} \frac{|k_m|}{2\pi} \frac{i\omega}{4P_m} \mathbf{V}_n(\varphi_n, z) \mathbf{V}_m(\varphi_m, d)^{*T} \mathbf{q}(x', y') \times \sqrt{\frac{2\pi}{|k_m R_m|}} e^{i\frac{\pi}{4} \operatorname{sgn}(-k_m)} e^{ik_m R_m}. \quad (16)$$

where,  $\varphi_m$  is the angle between the point where reflection arises and the source point relative to the edge normal. Likewise,  $\varphi_n$  is the angle between the calculation point and the reflection point.

Our goal is now to calculate  $G_{m,n}$ . The reflected wave  $n$  has the following form,

$$\mathbf{u}_r(x, y) = \sum_m \sum_n a_{m,n} \mathbf{V}_n(z). \quad (17)$$

Just before the reflection, for one path, the displacement field due to the incident mode  $m$  is given by,

$$\mathbf{u}_{dm}(x_p, y_p) = \left[ \frac{|k_m|}{2\pi} \frac{i\omega}{4P_m} \mathbf{V}_m(\varphi_m, z) \mathbf{V}_m(\varphi_m, d)^{*T} \mathbf{q}(x', y') \times \sqrt{\frac{2\pi}{|k_m R_m|}} e^{i\frac{\pi}{4} \operatorname{sgn}(-k_m)} e^{ik_m R_m} \right], \quad (18)$$

so just after the reflection, the displacement field can be expressed as

$$\mathbf{u}_{rm,n}(x_p, y_p) = \left[ r_{m,n} \frac{|k_m|}{2\pi} \frac{i\omega}{4P_m} \mathbf{V}_n(\varphi_n, z) \mathbf{V}_m(\varphi_m, d)^{*T} \mathbf{q}(x', y') \times \sqrt{\frac{2\pi}{|k_m R_m|}} e^{i\frac{\pi}{4} \operatorname{sgn}(-k_m)} e^{ik_m R_m} \right], \quad (19)$$

where  $r_{m,n}$  denotes the reflection coefficient related to the path  $m, n$  which will be calculated in section 4. At this stage, we have

$$G_{rm,n} = \sqrt{\frac{2\pi}{i}} r_{m,n} \frac{|k_m|}{2\pi} \frac{i\omega}{4P_m} \mathbf{V}_n(\varphi_n, z) \mathbf{V}_m(\varphi_m, d)^{*T}. \quad (20)$$

Finally, the displacement field after reflection can be expressed by:

$$\mathbf{u}_r = \sum_m \sum_n \left[ r_{m,n} \frac{|k_m|}{2\pi} \frac{i\omega}{4P_m} \mathbf{V}_n(\varphi_n, z) \mathbf{V}_m(\varphi_m, d)^{*T} \mathbf{q}(x', y') \right. \\ \left. \times e^{if_{m,n}(\gamma_m)} e^{i\frac{\pi}{4} \text{sgn}\left(\frac{\partial^2 f_{m,n}}{\partial \gamma^2} \Big|_{\gamma_m}\right)} \sqrt{\frac{2\pi}{|R_m k_m + \left(\frac{k_m \cos(\gamma)}{k_n \cos(\gamma_n)}\right)^2 R_n k_n|}} \right]. \quad (21)$$

In the next section, we will explain how efficiently taking into account efficiently the finite size of the source and how determining paths between it and the calculation points.

### 3. Finite-sized sources

#### 3.1. Fraunhofer-like approximation

In the isotropic case and for the direct field, the integral over the source surface can be accurately and efficiently evaluated thanks to Fraunhofer approximation. This approximation is based on a first order approximation of the phase term and a zero-th order approximation of the amplitude. Let  $(x_c, y_c)$ , denote the coordinates of the source centre. The direct displacement field given by Eq. 2 under Fraunhofer approximation writes

$$\mathbf{u}_d(x, y, z, \mathbf{q}) = \left( \sqrt{(x-x_c)^2 + (y-y_c)^2} \right)^{-1/2} \sum_m \frac{i\omega}{4P_m} \sqrt{\frac{|k_m|}{2\pi}} \mathbf{V}_m(\varphi_c, z) \mathbf{V}_m(\varphi_c, d)^{*T} \\ \times e^{i\frac{\pi}{4} \text{sgn}(-k_m)} e^{ik_m \sqrt{(x-x_c)^2 + (y-y_c)^2}} \iint_S \left[ e^{-ik_m \frac{xx'+yy'}{\sqrt{(x-x_c)^2 + (y-y_c)^2}} \mathbf{q}(x', y')} \right] dx' dy'. \quad (22)$$

The surface integral is easily calculated for standard geometries of source (rectangular or circular) generating in-plane or out-of-plane uniform stresses.

For example, considering rectangular and disk transducers generating uniform normal stress over their surface, the direct fields radiated into the plate by these sources are readily given by

$$\mathbf{u}_d(x, y, z, \mathbf{q}) = \left( \sqrt{(x-x_c)^2 + (y-y_c)^2} \right)^{-1/2} \sum_m \frac{i\omega}{4P_m} \sqrt{\frac{|k_m|}{2\pi}} \mathbf{V}_m(\varphi_c, z) \mathbf{V}_m(\varphi_c, d)^{*T} \\ \times e^{i\frac{\pi}{4} \text{sgn}(-k_m)} e^{ik_m \sqrt{(x-x_c)^2 + (y-y_c)^2}} F_m(x-x_c, y-y_c) \mathbf{q}(x_c, y_c). \quad (23)$$

$F_m$  is a modal function which stands for the result of the surface integral. For a rectangular-shaped transducer of aperture  $L_x \times L_y$  it is given by,

$$F_{m_{rect}}(\varphi_c) = L_x L_y \text{sinc}\left(k_m \frac{L_x}{2} \cos \varphi_c\right) \text{sinc}\left(k_m \frac{L_y}{2} \sin \varphi_c\right)$$



and for a disk-shaped transducer of radius  $a$ , by,

$$F_{m_{disk}} = \pi a^2 \frac{2J_1(k_m a)}{k_m a}.$$

As we can see, these expressions are only dependent on the angle  $\varphi_c$  between the source centre and the calculation point (at least in the case of a rectangular source). Since such an approximation is already valid before the reflection, it can be all the more used in the case of reflected paths taking into account the direction between the point where reflection arises and the centre of the source.

### 3.2. Paths between the source and the calculation points

The centre of the source is, as in the previous section  $(x_c, y_c)$ . The coordinates of the calculation point are denoted by  $(x, y)$ . We will search the coordinate of the reflection point  $(0, y_p)$  for a couple  $m, n$  of modes.

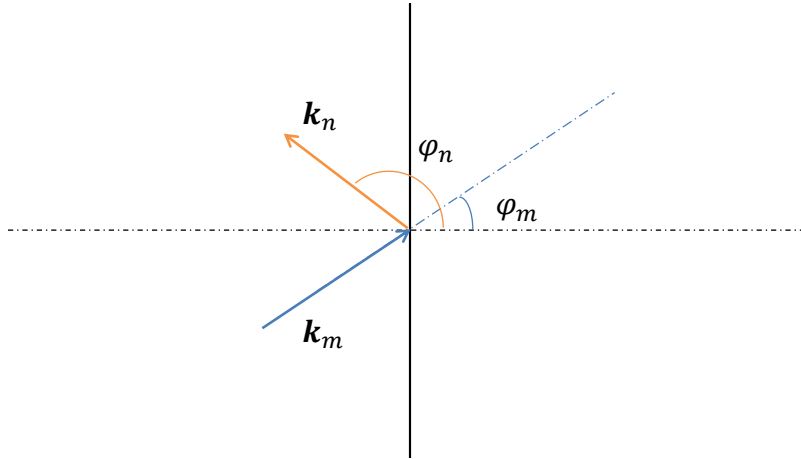


**Figure 3.** Reflection at an edge.

In an isotropic plate, the phase direction is the same as the energy direction. Denoting the incident angle by  $\varphi_m$  and the angle of reflection by  $\varphi_n$ , as shown on the figure 3, the Snell-Descartes' law gives us,

$$k_m \sin(\varphi_m) = k_n \sin(\varphi_n), \quad (24)$$

$$k_m \frac{y_p - y_c}{\sqrt{(y_p - y_c)^2 + x_c^2}} = k_n \frac{y - y_p}{\sqrt{(y - y_p)^2 + x^2}}, \quad (25)$$

After some algebra, we obtain the following polynomial to solve:

$$a_4 y_p^4 + a_3 y_p^3 + a_2 y_p^2 + a_1 y_p + a_0 = 0, \quad (26)$$

with

$$\begin{aligned} a_4 &= (k_m^2 - k_n^2) \\ a_3 &= -2(k_m^2 - k_n^2)(y_c + y) \\ a_2 &= (y_c^2 + 4y_c y + y^2)(k_m^2 - k_n^2) + x^2 k_m^2 - x_c^2 k_n^2 \\ a_1 &= -2((y_c y^2 + y_c^2 y)(k_m^2 - k_n^2) + x^2 y_c k_m^2 - x_c^2 y k_n^2) \\ a_0 &= (y_c y)^2 (k_m^2 - k_n^2) + (x y_c k_m)^2 - (x_c y k_n)^2. \end{aligned} \quad (27)$$

This polynomial has four roots. If a reflection point exists, it is the real solution where the value of  $y_p$  is between those of  $y$  and  $y_c$ . Now if we have a reflection point for a couple  $m, n$  of modes, we know the path for these between the source centre and the calculation point. For each of these paths, we must now calculate the reflection coefficients.

#### 4. Reflection coefficients

To calculate the reflection coefficients, we use the method proposed by Santhanam and Demirli [2]. In this method, stress free boundary conditions are assumed at the plate edge. For an incident mode  $m$  and all the reflected modes  $n$ , we can write the following system:

$$\begin{cases} \sigma_{11}^{(m)} + \sum_{n=1}^{\infty} r_{m,n} \sigma_{11}^{(n)} = 0 \\ \sigma_{12}^{(m)} + \sum_{n=1}^{\infty} r_{m,n} \sigma_{12}^{(n)} = 0 \\ \sigma_{13}^{(m)} + \sum_{n=1}^{\infty} r_{m,n} \sigma_{13}^{(n)} = 0 \end{cases} \quad . \quad (28)$$

In this system, all the stress tensors  $\sigma^{(i)}$  are written in the plate coordinate system. The SAFE method allows us to compute them in the propagation system. Therefore, in order to express them in the plate coordinate system, a transformation matrix must be introduced, as presented by Gunawan and Hirose [3]. The change of coordinate system is written as follows,

$$\sigma = Q \sigma_p Q^t, \quad (29)$$

where  $Q$  denotes the transformation matrix,  $\sigma_p$  denotes the stress expressed in the coordinate system attached to the wave propagation considered, and  $\sigma$  denotes the stress expressed in the plate coordinate system. The transformation matrix is readily given by:

$$Q = \begin{pmatrix} C & S & 0 \\ -S & C & 0 \\ 0 & 0 & 1 \end{pmatrix}. \quad (30)$$

We can see on the figure 3 that the incident mode makes an angle  $\varphi_m$  with respect to the plate frame. For this mode,

$$\begin{aligned} C_m &= \cos \varphi_m \\ S_m &= -\sin \varphi_m \end{aligned} \quad (31)$$

Now, the transformation matrices for the different reflected modes are similarly obtained by introducing the following notations:

$$\xi = k_m \sin \varphi_m \quad (32)$$

$$\mu = \pm \sqrt{k_n^2 - \xi^2} \quad (33)$$

$$C_n = -\frac{\mu}{k_n} \quad (34)$$

$$S_n = -\frac{\xi}{k_n} \quad (35)$$

Choose the sign in the Eq. (33) is made according to [3]. It must be noticed that for propagative modes,  $C_n$  and  $S_n$  are real valued. In these cases,  $Q$  is nothing but a rotation matrix and solving Eq. (26) leads to the obtaining of a reflection point.

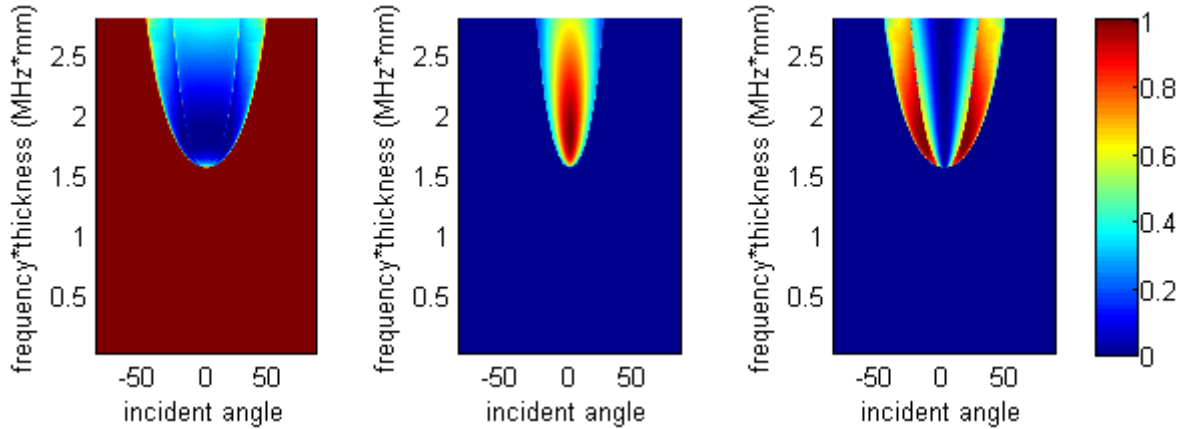


**Figure 4.** Energy reflection coefficient for A0 incident and for (from left to right) A0, A1, SH1 reflected.

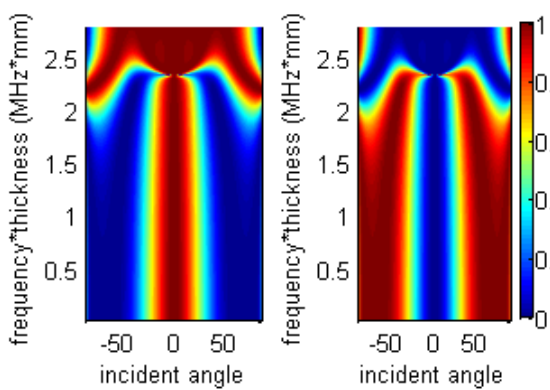


**Figure 5.** Energy reflection coefficient for S0 incident and for (from left to right) S0, SH0 reflected.

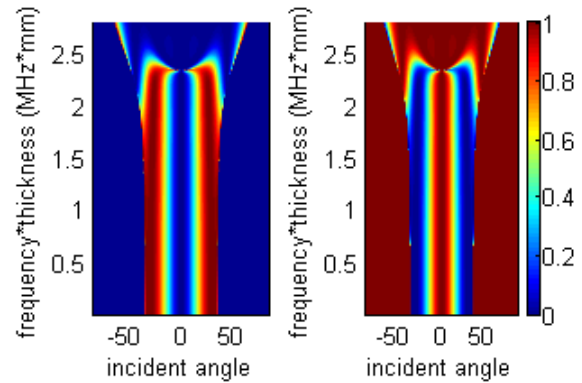


**Figure 6.** Energy reflection coefficient for SH0 incident and for (from left to right) S0, SH0 reflected.

Once all the stress tensors are written in the same coordinate system, we can calculate the  $r_{m,n}$  coefficients appearing in Eq. (28), by truncating the infinite sum over a finite number  $N$  of modes. All the propagative modes must be accounted for, together with a finite number of inhomogeneous and evanescent modes.

Energy reflection coefficients  $\mathcal{R}_{m,n}$  can also be computed likewise by means of,

$$\mathcal{R}_{m,n} = \frac{P_n}{P_m}(r_{m,n}r_{m,n}^*), \quad (36)$$

where  $P$  denotes the mean energy flux of the considered mode along the plate.

Figures 4, 5 and 6 present the energy reflection coefficients for the three first propagative modes as functions of the incident angle and of the frequency-thickness product. The plate considered in this simulation is made of aluminium and is 3 mm thick. Dispersion curves of propagative modes are plotted on Fig. 7.

Below the first cut-off frequency, the A0 mode is the only one propagative mode to present an antisymmetric shape. That is why an incident A0 mode is totally reflected as another A0 mode.

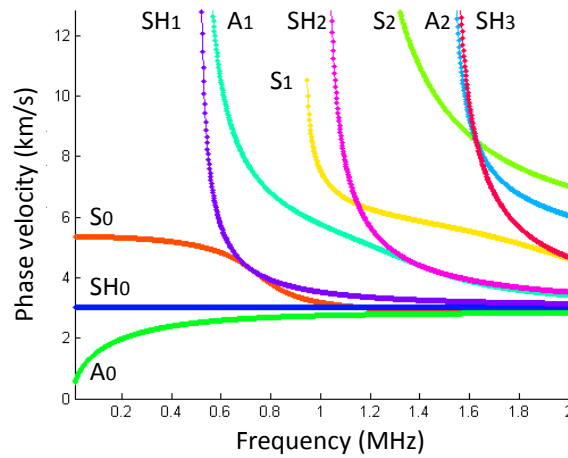


**Figure 7.** Dispersion curves of a 3-mm-thick aluminium plate.

Both the S0 and the SH0 modes have a symmetric shape. Therefore, when a S0 or a SH0 mode interacts with the free edge of the plate, mode conversion occurs.

## 5. Results in time domain

Throughout the theoretical derivations of field models described in previous sections, a single frequency excitation was assumed. In what follows, time-dependent wavefields are presented which are obtained by standard Fourier synthesis.

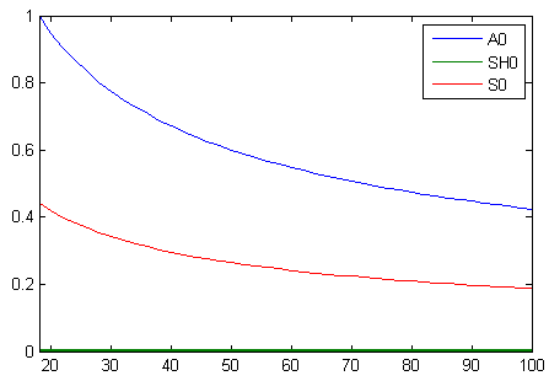


**Figure 8.** Normalized normal modal displacement along an axis from a distance of  $\lambda_{max}$  of the edge of the source centered at  $(0, 0)$ .

At first, we will compare the normal displacement due to each mode at the frequency of 400 kHz. As presented on Fig. 8, the A0 mode and the S0 mode are predominant while the SH0 mode is negligible.

In this simulation, we consider a 5-mm-diameter circular transducer centered at  $(-100, 0)$  which generates a normal uniform stresses excited by a toneburst of sine wave of 400 kHz centre frequency weighted by a Hanning window. We present on figure 9 the propagation of the waves with a reflection at four different times.

The first instant  $t = 18\mu s$  (a) was chosen before any reflection phenomenon occurs; calculation points reached by some acoustic energy are insonified only by direct contributions from the source. The second instant  $t = 31\mu s$  (b) was chosen at the beginning of the reflection process, when only the fastest mode reached the plate edge; interferences of direct and reflected contributions are visible close to the edge. The third instant  $t = 54\mu s$  (c) was chosen just after the slowest

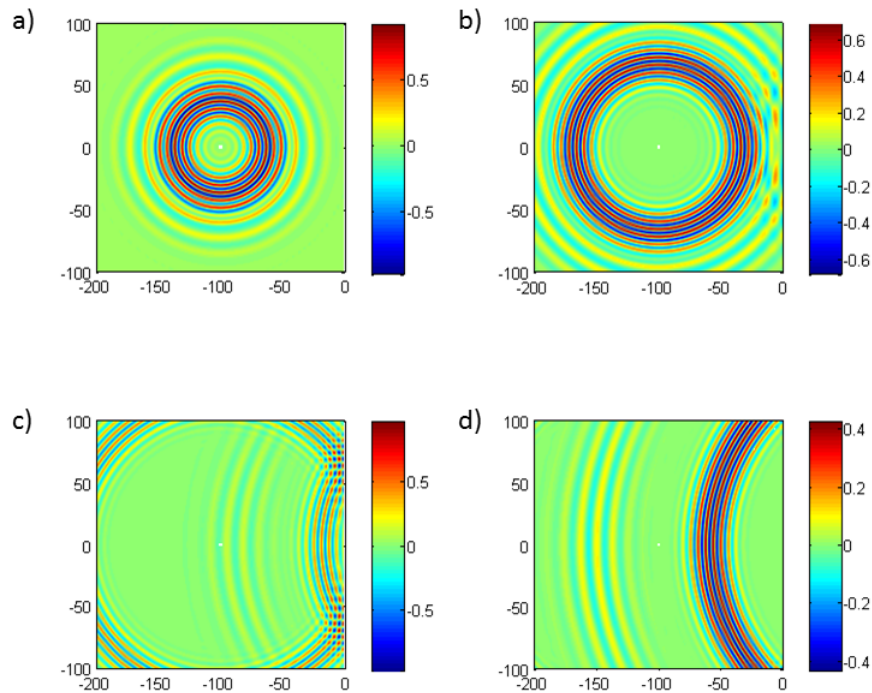


**Figure 9.** Four snapshots of the normal displacement associated to guided wave propagation in a plate with account of edge reflection (a) at  $18\mu s$ , (b) at  $31\mu s$ , (c) at  $54\mu s$ , and (d) at  $72\mu s$ .

contributions finished to reflect on the edge; at some calculation points, interferences with direct contributions are still visible. The last instant  $t = 72\mu s$  (d) was chosen when all the points of the computation zone are only insonified by waves reflected on the plate edge; there is no more interference.

The  $S_0$  mode is the fastest mode. So, it is the first to be reflected. Moreover, as expected we distinguish only the contribution of two modes.

## 6. Conclusion

An efficient model has been proposed to compute the elastic guided wave field radiated by finite-sized sources in a semi-infinite isotropic plate. The model gives the field at a point of the plate as the superposition of direct contributions from the source with contributions involving reflections onto the free edge of the semi-infinite plate. Modes are computed by means of the SAFE method but classical formulas for Lamb waves and transverse horizontal guided waves could be easily introduced. The calculation of reflected contributions is based upon the stationary phase method, stationary phase paths being easily determined by solving a simple polynomial equation. Fraunhofer-like approximation is used for efficiently evaluate the surface integral over transducer surface. This approximation was already known to combine efficiency and accuracy for the field radiated into an infinite plate [8]; this is all the more true for longer wavepaths involving edge reflection.

The recent article of Feng *et al.* [9] develops the mode-matching method for computing the scattering of obliquely incident guided waves by a straight feature. This method can be used straightforwardly in our model to deal with more complex boundary conditions at plate edges. Likewise, the integration along energy directions developed for predicting transducer diffraction

effects in anisotropic plates [8], could be adopted to generalize the present model to anisotropic cases.

## References

- [1] Raghavan A and Cesnik C E S 2005 *Smart Mater. Struct.* **14** 1448–1461
- [2] Santhanam S and Demirli R 2013 *Ultrasonics* **53** 271–282
- [3] Gunawan A and Hirose S 2007 *Mater. Trans.* **48** 1236–1243
- [4] Velichko A and Wilcox P D 2007 *J. Acoust. Soc. Am.* **121** 60–69
- [5] Taupin L, Lhémery A and Inquiétude G 2011 *J. Phys.: Conf. Ser.* **269** 012002
- [6] Stannes J J and Eide H A 1998 *J. Opt. Soc. Am. A* **15** 1285–1291
- [7] Stannes J J 1986 *Waves in focal regions* (CRC Press)
- [8] Stévenin M, Lhémery A and Grondel S 2016 *J. Phys.: Conf. Ser.* **684** 012004
- [9] Feng F, Shen Z and Shen J 2016 *Wave Motion* **60** 84–94